



Growth and oxidation of graphitic crystallites in soot particles within a laminar diffusion flame



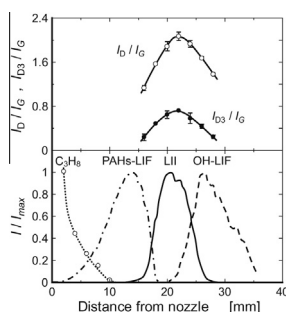
Kazuhiro Hayashida*, Shogo Nagaoka, Hiromi Ishitani

Department of Mechanical Engineering, Kitami Institute of Technology, 165 Koen-cho, Kitami, Hokkaido 090-8507, Japan

HIGHLIGHTS

- The soot nanostructure in the diffusion flame is investigated using Raman spectroscopy.
- The graphitic crystallite size of soot increase during the soot growth process.
- The graphitic crystallite size of soot decrease during the soot oxidation process.
- Soot formation and oxidation history within the flame affect the soot nanostructure.

GRAPHICAL ABSTRACT



ARTICLE INFO

Article history:

Received 4 January 2014

Received in revised form 27 February 2014

Accepted 6 March 2014

Available online 17 March 2014

Keywords:

Diffusion flame

Soot

Nanostructure

Raman spectroscopy

ABSTRACT

The growth and oxidation behaviors of graphitic crystallites in soot particles within a laminar co-flow propane diffusion flame were investigated experimentally. Soot was sampled along the flame axis and collected on a quartz–fiber filter. The soot nanostructure, i.e., the graphitic crystallite size and the amorphous carbon content in the soot particles, was characterized by Raman spectroscopy. The spatial distributions of the fuel, PAHs, soot and OH measured by laser diagnostic techniques are presented to examine the effect of the flame structure on the soot nanostructure. The Raman spectra of the soot show that both the graphitic crystallite size and the amorphous carbon content in the soot particles increase during the soot growth process. In addition, the crystallite size and the amorphous carbon content simultaneously decrease during the soot oxidation process by OH. HRTEM images of soot particles support that these findings obtained from the Raman spectroscopy are reasonable. The influences of the soot formation and oxidation history within the flame on the soot nanostructure are validated.

© 2014 Elsevier Ltd. All rights reserved.

1. Introduction

Soot emissions from such practical combustion devices as diesel engines, gas turbines and furnaces cause serious problems for the environment and human health. In addition, soot particles generated within combustion chambers reduce the durability of the combustion devices. Thus, an understanding of the mechanisms behind the inception, growth and oxidation of soot during

combustion is crucial for the development of soot-reduction strategies. These mechanisms have been investigated extensively over many years; nevertheless, the evolution of soot during combustion processes has not yet been fully understood, not only in practical combustion environments but also in simple laboratory flames.

Soot consists of small sub-micron particles that primarily contain carbon, and its internal nanostructure with respect to amorphous carbon, graphitic crystalline size and their arrangements might be related to the soot formation and growth conditions [1]. Vander Wal and Tomasek [2] investigated the differences in soot nanostructures based on formation and growth conditions

* Corresponding author. Tel./fax: +81 157 26 9206.

E-mail address: hayashka@mail.kitami-it.ac.jp (K. Hayashida).

by means of thermal pyrolysis of various hydrocarbons; their results clearly showed that the nanostructure of soot does depend on the initial fuel identity and the synthesis conditions. Similarly, Shaddix et al. [3] and Alfè et al. [4] showed that the soot nanostructure was affected by its formation chemistry and temperature history in the flames. It is well known that amorphous carbon is more reactive than crystalline carbon [5], and furthermore, the oxidative reactivity of crystalline carbon differs with the size, orientation and organization of the crystallite [6,7]. Thus, the oxidative reactivity of soot varies according to the soot nanostructure.

Raman spectroscopy is one characterization tool used to investigate the nanostructure of carbonaceous materials. Recently, correlation of such Raman spectroscopic parameters as peak positions, widths, and intensity ratios with the structure of disordered carbonaceous materials have been examined in detail [8–11], and valuable information on the carbon nanostructure can be obtained by analyzing the spectral profile of Raman scattering. Raman spectroscopy has been applied to characterize the nanostructure of soot emitted from practical combustion devices, and the relationship between the soot nanostructure and its oxidation reactivity has been examined [11–14].

Although the nanostructure of soot emitted from combustion devices is considered variable in terms of soot formation, growth and oxidation history within the flame, the processes of structural change in the soot nanostructure during combustion have not yet been fully understood. To clarify the effect of the soot growth and oxidation processes on the soot nanostructure, we examined the structural change in the soot nanostructure during combustion processes using a simple diffusion flame. The soot was sampled at different heights in the test flame, and its nanostructure was analyzed using Raman spectroscopy.

2. Experimental

2.1. Burner

The test flame used in this study was a laminar co-flow propane diffusion flame at atmospheric pressure. Propane was selected as the test fuel since propane is one of the most common gaseous fuels and its diffusion combustion yields the soot relatively dense within the flame [15,16]. The burner consisted of two concentric nozzles with inner diameters of 6 mm and 56 mm, and the fuel gas flowed through the inner nozzle. The flame length was defined as the distance from the nozzle rim to the luminous flame tip and was set to 30 mm. The fuel flow rate was set to 50 mL/min. To stabilize the flame, an annular airflow was supplied to the outer nozzle with a velocity of 0.5 m/s.

Axial velocity along the flame axis was calculated based on the buoyant acceleration of the flame gases given by Roper [17]. The acceleration due to buoyancy, a is assumed to be constant (25 m/s^2), and the axial velocity, U_z is given as [18]:

$$U_z = (U_{z0}^2 + 2az)^{1/2}, \quad (1)$$

where U_{z0} is flow velocity of fuel at the nozzle exit. Cumulative residence time of soot particles within the flame, τ_z , along the axial streamline was obtained from the following equation:

$$\tau_z = \int_0^z \frac{dz}{U_z}. \quad (2)$$

2.2. Soot sampling

Soot-containing combustion gas was sucked out of the flame via iso-kinetic sampling by means of a stainless-steel probe inserted vertically into the flame, and the soot was collected on a quartz-fi-

ber filter. Santamaría et al. [19,20] confirmed that the soot particles sampled by the stainless-steel probe had the same properties with that of a quartz probe. Thus, the catalytic effects on soot properties were expected to be negligible small in the process of soot sampling. The soot sampling was performed on the flame axis between $z = 16 \text{ mm}$ and 28 mm . Suction rate was controlled with a needle valve and syringe system [16], and was set between 21 mL/min (distance from the nozzle $z = 16 \text{ mm}$) and 27 mL/min ($z = 28 \text{ mm}$). The soot deposited on the sampling probe was periodically burnt off by another blue flame, and furthermore, soot residue in the probe inner wall after the sampling was removed before each measurement. The probe with an outer diameter of 1.0 mm and an inner diameter of 0.7 mm caused little or no visible disturbance. However, this inner diameter might be somewhat large with respect to the luminous flame width near the flame tip ($\sim 2.2 \text{ mm}$). Therefore, soot particles sampled near the flame tip might partially include soot formed around the flame axis.

2.3. Soot characterization

The soot nanostructure was characterized using Raman spectroscopy. Fig. 1 shows a schematic of the Raman spectroscopy system. This system consisted of an Ar^+ laser (NEC, GLG3202) and a spectrograph (Horiba Jobin Yvon, iHR320) fitted with a CCD camera (Hamamatsu photonics, C704). A laser wavelength of 488 nm was applied for the Raman spectroscopy, and a laser line filter was used to attenuate the background plasma line contained in the laser light. To avoid modification of the soot nanostructure due to laser-induced heating effects [21], a defocused laser beam was applied to the soot sample on the quartz-fiber filter. Scattered light from the sample was collected in the backscattering configuration with an incident beam perpendicular to the sample surface. The Raman spectrum was captured by the CCD camera through the spectrograph. The grating of the spectrograph contained 1200 grooves/mm , and the entrance slit of the spectrograph was set at $700 \mu\text{m}$, producing a spectral resolution of 1.6 nm . A notch filter was placed in front of the spectrograph to eliminate the Mie scattering component.

Morphology of soot particles was evaluated by means of high-resolution transmission electron microscopy (HRTEM). Soot samples on the quartz-fiber filter were ultrasonically dispersed in ethanol, and then a droplet of the colloidal solution was placed on a lacey carbon film coated TEM grid. The grid and sample was dried in the atmosphere. Soot particles were observed by a field-emission transmission electron microscope (JEOL, JEM-2010F) operated at 200 kV with point resolution of 0.19 nm .

2.4. Spectral analysis of soot via Raman spectroscopy

Fig. 2 shows a typical Raman spectrum of soot. Soot was sampled at a distance from the nozzle $z = 16 \text{ mm}$ in the test flame on

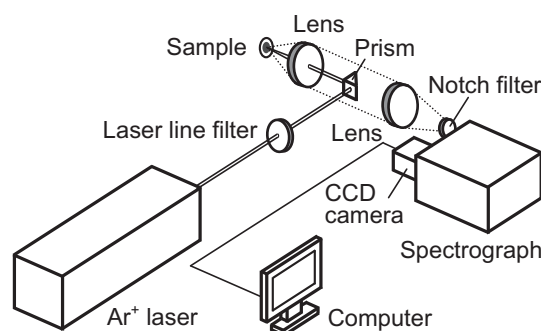


Fig. 1. Schematic illustration of the Raman spectroscopy system.

Download English Version:

<https://daneshyari.com/en/article/6637570>

Download Persian Version:

<https://daneshyari.com/article/6637570>

[Daneshyari.com](https://daneshyari.com)